

# 1 SARS-CoV-2 infection drives a glycan switch of peripheral T cells at 2 diagnosis.

3 Inês Alves<sup>1,2,3§</sup>, Manuel M. Vicente<sup>1,2,4§</sup>; Joana Gaifem<sup>1,2</sup>, Ângela Fernandes<sup>1,2</sup>, Ana M. Dias<sup>1,2</sup>,  
4 Cláudia S. Rodrigues<sup>1,2</sup>, José Carlos Oliveira<sup>5</sup>, Nair Seixas<sup>6</sup>, Luis Malheiro<sup>7</sup>, Miguel A. Abreu<sup>4,8</sup>;  
5 Rui Sarmiento e Castro<sup>4,8</sup>; Salomé S. Pinho<sup>1,2,3,4,9\*</sup>

6 <sup>1</sup> Institute of Molecular Pathology and Immunology, University of Porto (IPATIMUP), 4200-135 Porto, Portugal

7 <sup>2</sup> i3S – Institute for Research and Innovation in Health, University of Porto, 4200-135 Porto, Portugal.

8 <sup>3</sup> Faculty of Medicine, University of Porto, 4200-319 Porto, Portugal.

9 <sup>4</sup> Institute of Biomedical Sciences Abel Salazar (ICBAS), University of Porto, 4050-313 Porto, Portugal.

10 <sup>5</sup> Department of Clinical Pathology, Centro Hospitalar Universitário do Porto, 4099-001 Porto, Portugal.

11 <sup>6</sup> Department of Clinical Pathology, Centro Hospitalar Vila Nova de Gaia/Espinho, 4434-502 Gaia, Portugal

12 <sup>7</sup> Department of Infectious Diseases, Centro Hospitalar Vila Nova de Gaia/Espinho, 4434-502 Gaia, Portugal

13 <sup>8</sup> Department of Infectious Diseases, Centro Hospitalar Universitário do Porto, 4099-001 Porto, Portugal.

14 <sup>9</sup> Lead Contact

15 §These authors contributed equally

16 \*Corresponding author: [salomep@ipatimup.pt](mailto:salomep@ipatimup.pt) (S.S.P)

17  
18 **Grant Support:** The Institute of Molecular Pathology and Immunology of the  
19 University of Porto integrates the Institute for Research and Innovation in Health (i3S)  
20 research unit, which is partially supported by the Portuguese Foundation for Science  
21 and Technology (FCT). This article was partially funded by the FCT, in collaboration  
22 with the Portuguese Agency for Clinical Research and Biomedical Innovation (AICIB)  
23 under the special funding, “RESEARCH 4 COVID-19”\_Project #006 granted to the PI  
24 Salomé S. Pinho. IA [SFRH/BD/128874/2017] and MV [PD/BD/135452/2017]  
25 received funding from the FCT.

26 **Running Title:** T cell glycan switch in SARS-CoV-2 infection

## 27 Abstract

28 COVID-19 is a highly selective disease in which SARS-CoV-2 infection can result in  
29 different clinical manifestations ranging from asymptomatic/mild to severe disease that  
30 requires hospitalization. Here, we demonstrated that SARS-CoV-2 infection results in a  
31 glycosylation reprogramming of circulating lymphocytes at diagnosis. We identified a  
32 specific glycosignature of T cells, defined upon SARS-CoV-2 infection and apparently  
33 triggered by a serological factor. This specific glycan switch of T cells is detected at  
34 diagnosis being more pronounced in asymptomatic patients. We further demonstrated  
35 that asymptomatic patients display an increased expression of a viral-sensing receptor,  
36 through the up-regulation of DC-SIGN in monocytes. We showed that higher levels of  
37 DC-SIGN in monocytes at diagnosis correlates with better COVID-19 prognosis. These

38 **NOTE:** This preprint reports new research that has not been certified by peer review and should not be used to guide clinical practice.  
new evidences pave the way to the identification of a novel glycan-based response in T

39 cells that may confer protection against SARS-CoV-2 infection in asymptomatic  
40 patients, highlighting a novel prognostic biomarker and potential therapeutic target.

41 **Keywords:** asymptomatic / DC-SIGN / glycan-recognition receptors / *N*-glycosylation /  
42 prognosis / SARS-CoV-2 / T-cell activation

43

## 44 **Introduction**

45 Coronavirus SARS-CoV-2 is the etiologic agent responsible for the global pandemic of  
46 Coronavirus disease 2019 (COVID-19), that, as of 9<sup>th</sup> of February, has infected over  
47 106 million people worldwide(1, 2). The overall mortality of COVID-19 is between  
48 0.5% and 3.5%(1, 2). COVID-19 is a highly selective disease. In fact, only some  
49 infected individuals get sick, and although most of the critically ill are elderly, some  
50 patients that die are previously healthy and/or relatively young(3). There is an urgent  
51 need to improve the understanding of the pathophysiology of this disease, envisioning  
52 better management in terms of patients care, treatment options, vaccination strategies  
53 and the allocation of healthcare resources. Vaccine development against SARS-CoV-2  
54 poses a great promise for the resolution of the pandemic, and several vaccines are now  
55 being distributed among the world population, namely mRNA- and protein-based  
56 approaches(4, 5). However, its long-term protection, effectiveness to re-infection,  
57 efficacy to new variants and availability for the general public is still on trial. This lack  
58 of knowledge highlights the importance of understanding patient-specific immune  
59 response to infection, envisioning the identification of novel mechanisms of disease.  
60 Moreover, comprehensive insights on COVID-19 molecular mechanism may be  
61 translated into diagnostic or prognostic biomarkers, therapeutic targets to improve  
62 patient's clinical management and patients' stratification for vaccination.

63 SARS-CoV-2 infection results in a broad range of symptoms(6). Several studies on  
64 immune profiling of infected patients consistently revealed an immunological  
65 dysregulation, observed in peripheral blood mononuclear cells (PBMCs). A decrease of  
66 T cells and dendritic cells frequencies and an increase of monocytes and neutrophils  
67 have been observed in hospitalized infected individuals, as well as a cytokine  
68 dysregulation, the so-called "cytokine storm" associated with critical illness(7–10).

69 However the mechanism underlying this immunological dysregulation remains largely  
70 unknown.

71 Despite overlooked, the field of glycobiology can provide missing answers to  
72 immunological questions. Glycosylation is a major post-translational mechanism  
73 characterized by the enzymatic addition of glycans (carbohydrates) to proteins or lipids  
74 of essentially all cells, including immune cells. In fact, glycans are master regulators of  
75 immune cell functions, defining the activation and differentiation of T cells(11, 12). In  
76 the cellular immune system, we and others have previously demonstrated the regulatory  
77 power of glycans in adaptive immune response through the modulation of T cell  
78 activation thresholds associated with the immunopathogenesis of autoimmune diseases  
79 and cancer(13–19). Moreover, being present in several pathogens, glycans can also be  
80 sensed by immune cells, through their recognition by specific glycan-recognizing  
81 receptors expressed in those cells(20). Like the majority of viruses, SARS-CoV-2 viral  
82 capsids are also covered with glycans. More specifically, the spike protein of the SARS-  
83 CoV-2 envelope was shown to be highly glycosylated (harboring 22 *N*-glycosylation  
84 sites) with glycan structures such as oligomannose and some branched *N*-glycans(21,  
85 22). These structures can be specifically recognized by glycan binding proteins (GBPs)  
86 of host's immune cells, such as the C-type-lectin Dendritic Cell-Specific Intercellular  
87 adhesion molecule-3-Grabbing Non-integrin (DC-SIGN), present in innate immune  
88 cells, promoting virus recognition and elimination(23, 24).

89 Defining the glycosylation profiles of immune cells in SARS-CoV-2 infected  
90 individuals and how they impact their effector functions remains completely unknown,  
91 being of utmost importance for the understanding of COVID-19 immunopathogenesis,  
92 as well as for the improvement of the clinical management of the disease and for  
93 pandemic control measures, namely as a stratification biomarker.

94 In this study, we discovered that circulating T cells exhibit a glycan switch upon SARS-  
95 CoV-2 infection that is detected at COVID-19 diagnosis. This change in the  
96 glycosylation profile of T cells appears to be triggered by a serum inflammatory factor  
97 present in infected patients. This specific T cell glycan switch is more pronounced in  
98 asymptomatic patients, rather than in those who exhibit symptoms. Importantly from a  
99 clinical standpoint, we also unveiled that COVID-19 patients with good prognosis  
100 exhibit an upregulation of DC-SIGN expression in circulating monocytes.

101

## 102 **Material and Methods**

### 103 **Cohort description and patient's selection criteria**

104 The present study integrates a total of 32 patients diagnosed with SARS-CoV-2  
105 from 2 individual Portuguese cohorts (between May 2020 and July 2020), 20 patients  
106 from Infectious Disease Department, Centro Hospitalar e Universitário do Porto  
107 (CHUP), Porto, Portugal and 12 patients from Infectious Disease Department, Centro  
108 Hospitalar de Vila Nova de Gaia/Espinho (CHVNG), Vila Nova de Gaia, Portugal. The  
109 total cohort includes patients of both genders and age between 22 and 89 years old. All  
110 the samples were included in all the FACS analysis discussed.

111 Blood was collected and plasma and PBMCs were isolated at the time of  
112 diagnosis and 14 days (n=6) after diagnosis. Similar analysis was conducted in a subset  
113 of patients (n=2) that recovered.

114 The eligibility criteria for inclusion in this study were SARS-CoV-2 positive  
115 patients asymptomatic or symptomatic with different levels of severity (mild, moderate  
116 and severe). Asymptomatic patients (n=5) were defined as positive for the SARS-CoV-  
117 2 PCR test, but no signs of diseases. The following criteria were used to stratify  
118 symptomatic SARS-CoV-2 patients in terms of the disease severity and accordingly  
119 with WHO guidelines (25); 1- MILD (n=18): individuals with no evidences of  
120 pneumonia; 2- MODERATE (n=6): individuals without need of invasive mechanical  
121 ventilation and without need of admission to hospital intensive care unit, but evidence  
122 of pneumonia and need of supplemental oxygen; 3- SEVERE (n=1): individuals with  
123 need of invasive mechanical ventilation and with need of admission to hospital  
124 intensive care unit. Patients demographic and relevant clinical data are summarized in  
125 table 1.

126 Healthy controls (n=5) are represented by volunteer individuals with no history  
127 of infection disorders that underwent CHUP for routine analysis.

128 All participants gave informed consent about all clinical procedures and research  
129 protocols were approved by the ethics committee of CHUP and CHVNG, Portugal.

130

### 131 **Human PBMCs isolation**

132 Human peripheral blood mononuclear cells (PBMCs) from COVID-19 patients and  
133 healthy donors were isolated by gradient centrifugation using 1 volume of  
134 Lymphoprep<sup>TM</sup> (Stemcell Technologies) for 2 volumes of blood, 30 minutes at 900 x g  
135 with the brake off. The upper phase, containing the serum, was collected and stored at -  
136 80°C. PBMCs (interphase) were collected, washed twice with PBS and incubated with  
137 FVD-APC-eFluor780 (eBioscience) for 30 minutes. Cells were washed with PBS, fixed  
138 with 2% formaldehyde (PanReac ApplieChem) and resuspended in FACS buffer (PBS  
139 2%FBS). All procedures were performed under biosafety level 3 (BSL3) conditions.

#### 140 **Flow Cytometry Staining**

141 For lectin staining, cells were incubated with conjugated lectins (Vector  
142 Laboratories): Phaseolus Vulgaris leucoagglutinin (L-PHA-fluorescein, FITC),  
143 Galanthus Nivalis lectin (GNA-fluorescein, FITC), biotinylated Sambucus Nigra lectin  
144 (SNA) and biotinylated Aleuria aurantia lectin (AAL) for 15 minutes. Biotinylated  
145 lectins were incubated with streptavidin-PE-Cy7 (eBioscience) for 30 minutes. For  
146 surface marker staining, cells were stained for 30 minutes on ice while protected from  
147 light with the following antibodies: APC anti-human TCR $\gamma\delta$  (clone B1), BV510 anti-  
148 human CD69 (clone FN50), PE anti-human CD25 (clone BC96), BV421 anti-human  
149 CD14 (clone 63D3), PE anti-human CD56 (clone HCD56), PE-Cy7 anti-human CD206  
150 (clone 15-2) from Biolegend; eFluor<sup>TM</sup> 450 anti-human CD4 (clone RPA-T4), PerCP-  
151 eFluor<sup>TM</sup> 710 anti-human PD-1 (clone J105), PE-Cy5 anti-human CD19 (clone HIB19),  
152 eFluor<sup>TM</sup> 450 anti-human IgM (clone SA-DA4), eFluor<sup>TM</sup> 660 anti-human galectin 3  
153 (clone M3/38), APC anti-human CD11c (clone BU15), PE-Cy5 anti-human CD86  
154 (clone IT2.2) from eBioscience; PE anti-human TCR $\alpha/\beta$  (clone BW242/412) from  
155 Miltenyi; BV510 anti-human CD3 (clone OKT3) from BD Biosciences; for DC-SIGN  
156 staining, cells were incubated with DC-SIGN rabbit IgG (Biorad) followed by  
157 incubation with polyclonal swine anti-rabbit IgG (FITC; Dako) for 30 minutes on ice.  
158 Cells were resuspended in FACS buffer prior analysis. Data were obtained on a BD  
159 FACS Canto II instrument (Becton Dickinson) and analyzed using FlowJo v10.0 (Tree  
160 Star Inc.).

#### 161 ***In vitro* assessment of glycan modulation of T cells**

162 PBMCs from healthy and independent from the COVID-19 cohort human donors  
163 were isolated from fresh collected blood, as described above. PBMCs were cultured in

164 RPMI-1640 (Gibco) supplemented with 10% (v/v) heat-inactivated fetal bovine serum,  
165 1% penicillin/streptomycin and 10% of plasma from 4 asymptomatic or moderate  
166 patients, for each condition. Different cell culture conditions were tested, namely human  
167 plasma concentration (25% and 10%) as well as time of culture (4 days, 2 days, 24h and  
168 12h). The optimal culture condition (with lower cell death and stronger glycan  
169 modulation) was selected (10% human plasma and 24h cell culture). After 24h cell  
170 glycoprofile was evaluated using the same antibodies and lectin panel selected above.  
171 Data were obtained on a BD FACS Canto II instrument (Becton Dickinson) and  
172 analyzed using the FlowJo 10.0 software (Tree Star Inc.).

173

#### 174 **Data visualization and statistical analysis**

175 Data visualization and statistical analyses (non-parametric Mann-Whitney t-test)  
176 were done using GraphPad Prism 9 software.

177 The prediction capacity of DC-SIGN levels to discriminate patients who develop a  
178 poor disease course from those that have a good disease course was determined by  
179 plotting the receiver operating characteristic (ROC) curves and calculating the area  
180 under the curve (AUC). The cut-off that revealed the best balance between sensitivity  
181 and specificity was selected for the subsequent statistical analysis. Sensitivity,  
182 specificity, and positive and negative predictive values were calculated. Univariate  
183 binary logistic regression analysis was performed to test DC-SIGN levels and disease  
184 progression (good: asymptomatic maintained asymptomatic and/or severity decreased at  
185 least one category; poor: symptoms were not improved and/or escalate to a higher  
186 severity). In logistic regression, model goodness-of-fit was assessed by the Hosmer-  
187 Lemeshow statistic and test. Results are presented as odds ratios (ORs) for each  
188 category as compared with a predefined reference category, and their respective 95%  
189 confidence intervals (CIs). Odds ratios above one and below one are indicative,  
190 respectively, of higher and lower odds of develop poor disease course as compared with  
191 a reference category. Statistical analysis was performed using the statistical software  
192 SPSS version 25 (IBM Corp., IBM SPSS Statistics for Windows, Version 25.0,  
193 Armonk, NY; released 2017) The threshold used for statistical significance was  $p$ -  
194 value < 0.05.

195 **Results**

196 **SARS-CoV-2 infected individuals display decreased  $\beta$ 1,6-GlcNAc branched and**  
197  **$\alpha$ 2,6-sialic acid *N*-glycans on peripheral T cells at diagnosis.**

198 Taking into consideration the fact that it is still unclear the underlying mechanisms that  
199 explain a differential inter-individual clinical presentation of COVID-19 at diagnosis,  
200 we herein characterized the glycosylation profile of T cells from patients' peripheral  
201 blood. A lectin-based flow cytometry of the T cell populations was performed to  
202 evaluate glycosylation profiles. We started by analysing the levels of expression of  
203  $\beta$ 1,6-GlcNAc branched *N*-glycan structures, known to have a major impact on the  
204 regulation of T cell activity and function(13, 16, 26), using the L-PHA lectin. Our  
205 results demonstrated that, overall, T cells from infected (IF) subjects have a decrease in  
206 branched *N*-glycan structures, particularly on CD8<sup>+</sup> and  $\gamma\delta$  T cells, when compared to  
207 non-infected (non-IF) ones (Figure 1A, top and bottom left panel). Moreover, T cells  
208 from asymptomatic patients have lower levels of  $\beta$ 1,6-GlcNAc branched *N*-glycans, that  
209 gradually tend to increase along disease severity (**Figure 1A, right**). Notably, CD8<sup>+</sup> T  
210 cells display a significant decrease in the levels of expression of complex branched *N*-  
211 glycans in asymptomatic and mild disease patients, when compared to non-IF  
212 individuals (**Figure 1A, top**).

213 Concerning  $\alpha$ 2,6-sialylation (recognized by the SNA lectin), already described to play a  
214 role in the regulation of T cells immune response(27), our results demonstrate that  
215 CD8<sup>+</sup> T cells from IF patients display a significant decreased SNA binding, in  
216 comparison with non-IF individuals (**Figure 1B, top left**). Consistently, asymptomatic  
217 patients present the lowest levels of SNA binding compared to non-IF (Fig.1B, top  
218 right). Even though the levels of SNA binding were shown to be associated with age  
219 (**Supplemental Figure 1E**), there are no significant differences between the mean age  
220 of asymptomatic and symptomatic patients (**Supplemental Table 1**). Curiously, for  
221 both glycans, the two COVID-19 convalescent patients seem to recover (or surpass) the  
222 levels of expression of  $\beta$ 1,6-GlcNAc branched and  $\alpha$ 2,6-sialic acid glycan structures in  
223 all T cell subsets (**Fig. 1A and B, right**). These results showed that CD8<sup>+</sup>T cells from  
224 asymptomatic patients display a defect in branched and sialylated *N*-glycans when  
225 compared with non-IF.

226 The differences observed in the glycosylation profile of T cells across severity, were not  
227 related to the abundance or activation of T cell populations, since CD3<sup>+</sup>, CD4<sup>+</sup>, CD8<sup>+</sup>  
228 and  $\gamma\delta$  T cells showed similar frequencies as well as similar levels of PD1 and CD69  
229 expression between the groups, with the exception of lowered CD3<sup>+</sup> population and  
230 increased CD69<sup>+</sup> within CD8<sup>+</sup> T cells, in the mild disease group (**Supplemental Figure**  
231 **1A, B and C**).

232 In addition, and since glycosylation is a dynamic process that can change along with  
233 disease status, we took advantage of a limited longitudinal follow-up analysis using a  
234 single patient, representative of each severity group (asymptomatic, mild, moderate and  
235 severe), which revealed that levels of expression of  $\beta$ 1,6-GlcNAc and  $\alpha$ 2,6-sialylation  
236 are restored in patients that improved disease severity at day 14 post-diagnosis  
237 (**Supplemental Figure 1D**).

238 No major differences were observed for other glycan structures such as fucosylation  
239 (AAL binding) or mannosylation (GNA binding) in the different T cell subsets at  
240 diagnosis (**Supplemental Figure 1A and B**).

241 These results showed that SARS-CoV-2 infected individuals led to an *en bloc* decreased  
242 expression of specific glycan structures such as  $\beta$ 1,6-GlcNAc branched *N*-glycans and  
243  $\alpha$ 2,6-sialic acid in T cells, predominately in CD8<sup>+</sup> T cells and asymptomatic patients.  
244 The absence of differences on high mannose structures (GNA binding) or fucose  
245 residues on T cells (AAL binding), support the specificity of the glycan switch. In fact,  
246 decreased levels of  $\beta$ 1,6-branched *N*-glycans in T cells have been pointed out as a  
247 mechanism of TCR threshold regulation, by hampering the TCR complex clustering and  
248 lowering the necessary amount of antigen-recognition to signal a cellular response(28).  
249 Moreover, surface  $\alpha$ 2,6-sialylation also regulates T cell immune response through  
250 galectins binding modulation(29–31).

251 In order to further clarify the underlying mechanism that imposes the changes in the  
252 glycosylation profile of circulating T cells upon SARS-CoV-2 infection, we have  
253 performed an *in vitro* assay, in which PBMCs isolated from healthy individuals were  
254 co-cultured with plasma from 4 patients from either each group: non-IF, asymptomatic  
255 or moderate disease. Our results showed that T cells, upon co-culture with plasma from  
256 asymptomatic patients displayed a significant decreased expression of  $\beta$ 1,6-GlcNAc  
257 branched *N*-glycans (**Figure 2A**) and  $\alpha$ 2,6-sialylation (**Figure 2B**), when compared to T

258 cells cultured with plasma from non-IF individuals and moderate disease patients. These  
259 results suggest the existence a specific serum factor that in asymptomatic patients drives  
260 a remarkable drop of complex branched and sialylated glycans structures on T cells. In  
261 fact, it is known that asymptomatic patients display a differential serum composition of  
262 cytokines and chemokines, when compared to symptomatic (32, 33). Moreover, T cell  
263 glycosylation is known to be modulated by specific interleukins, namely IL-2 and IL-7  
264 that regulate the transcription of specific Golgi glycosyltransferases(17, 25), which  
265 renders the hypothesis that an extracellular factor could be mediating the T cells glycan  
266 switch in a more efficient manner in asymptomatic than symptomatic patients.

267

### 268 *Levels of DC-SIGN expression in circulating monocytes predict COVID-19 prognosis*

269 To gain further insights in the viral-glycan recognition mechanism, we have  
270 characterized the expression of specific GBPs expressed by innate immune cells that are  
271 known to sense and recognize specific viral glycans, instructing an immune  
272 response(34). Regarding the abundance of innate cells, we have observed an increase in  
273 the frequency of dendritic cells (DCs) as well as monocytes (Mo) in asymptomatic  
274 patients, when compared to Non-IF individuals, and no differences in terms of NK and  
275 NK-T cells subsets (**Supplemental Figure 1B**). Regarding their activation state,  
276 analysed by CD86 expression, only monocytes are shown to be activated in  
277 asymptomatic and mild disease patients (**Supplemental Figure 1C**). This is in  
278 accordance with previous findings(35).

279 Specifically, DC-SIGN, a C-type-lectin that recognizes mannose structures, is already  
280 known to play a role in the SARS-COV-2 recognition(24), being expressed by  
281 monocytes, immature DCs and macrophages. Our results showed that patients from the  
282 asymptomatic group displayed higher levels of DC-SIGN expression in monocytes  
283 compared moderate disease (**Figure 3A**), suggesting an increased capacity of  
284 asymptomatic patients to sense and recognize the virus.

285 Taking into consideration the biological relevance of DC-SIGN expression in  
286 monocytes as the first sensing mechanism upon SARS-CoV-2 infection, and given the  
287 heterogenous expression of DC-SIGN among infected individuals (at diagnosis),  
288 (Figure 3A) we next analysed its prognostic value. A longitudinal cohort was used with

289 clinical information in terms of disease progression (development of a poor *versus* good  
290 prognosis at day 14 post-diagnosis, characterized in Supplementary Table 1).  
291 Remarkably, the expression levels of DC-SIGN in monocytes were found to be able to  
292 stratify patients at diagnosis in terms of their likelihood of developing a good versus a  
293 poor disease prognosis with a specificity and sensitivity of 78.9% and 63.6%,  
294 respectively (**Figure 3B**). The univariate analysis demonstrated that high levels of DC-  
295 SIGN expression in monocytes at diagnosis increase the odds ratio (OD) associated  
296 with the prediction of having a good prognosis,  $OD = 6.548$   $p$ -value = 0.011. In fact, the  
297 recognition of the coronaviruses' glycans by innate immune cells was demonstrated to  
298 be mediated by DC-SIGN(23, 24). An increased expression of this C-type-lectin at the  
299 initial days of infection suggests a more efficient viral recognition and subsequent  
300 clearance, resulting in a good prognosis of the disease.

301

## 302 **Discussion**

303 Our results demonstrated for the first time that SARS-CoV-2 infection imposes a  
304 glycosylation reprogramming of adaptive immune cells suggesting a specific glycan  
305 switch of T cells that may define their ability to successfully deal with infection. We  
306 identified a specific glycosylation signature of circulating T cells that is associated with  
307 their activity and function, distinguishing infected patients from non-infected  
308 individuals. Our results also suggest that the glycan switch imprinted in circulating T  
309 cells could be mediated by a serum extracellular factor(s), occurring just after SARS-  
310 CoV-2 infection (**Supplemental Figure 2**). In fact, previous evidences from others and  
311 us demonstrated that the deficiency in branched *N*-glycan structures on T cells imposes  
312 a hyper-reactive phenotype with decreased threshold of T cell activation and increased  
313 T cell activity(13, 28). We herein propose that the immune response against SARS-  
314 CoV-2 infection appears to be influenced by the glycosylation profile of circulating T  
315 cells which defines their effective functions. In fact, a pronounced deficiency of  
316 complex branched and sialylated glycans on CD8<sup>+</sup> and  $\gamma\delta$  T cells were observed in  
317 asymptomatic COVID-19 patients. This dynamic and plastic glycoimmune modulation  
318 ("Glyco-Immune Alert" mechanism) may constitute a novel mechanism of host-  
319 response, that contributes to further understand the immunological differences among  
320 infected individuals(36).

321 Furthermore, we also showed another glycan-based mechanism of host response to  
322 SARS-CoV-2 driven by the upregulation of the viral's glycans recognizing receptor  
323 DC-SIGN in monocytes, with prognostic application when detected at diagnosis.

324 This study unlocks the identification of a specific glycosignature of T cells as well as a  
325 prognostic biomarker in COVID-19. Further studies are needed to explore the  
326 mechanistic impact of the T cell glycan switch in infection and along disease course.  
327 Moreover, it is fundamental to identify the critical serological factor(s) that instructs this  
328 T cells glyco-reprogramming, as a potential new biomarker and therapeutic target. Our  
329 study was conducted during the first wave of COVID-19 (March-July 2020) having a  
330 limitation in terms of sample size, indicating the need to validate these promising  
331 observations in larger and well-characterized multicentric cohorts as well as analysing  
332 the impact of other SARS-CoV-2 variants in T cells glycan switch.

333 These new evidences in COVID-19 pave the way to the identification of a specific  
334 blood glycosignature able to stratify patients at diagnosis according with their risk to  
335 evolve to worsen disease. This will certainly contribute to improve vaccination strategy  
336 and patients risk stratification, optimizing an effective allocation and management of  
337 health care resources such as ventilators and intensive care facilities.

338 **Acknowledgments:** We would like also to thank to all the Portuguese clinicians  
339 involved in COVID-19 patients 'care, with a special thanks to those from CHUP and  
340 CHVNG that directly or indirectly contributed to this work (Dr. Tiago Teixeira from  
341 CHVNG) and to all the patients that accepted to participate in this study. We also  
342 acknowledge the nurses and technicians that collaborated in the collection of the  
343 samples, especially Nurse Teresa Cruz from CHUP.

344 **Author contributions:** IA, MV and SSP designed research. IA, MV, JG, AF, AMD and  
345 CSR performed research. SSP contributed new reagents/analytical tools. NS, LM, MAA  
346 and RSC provided and characterized clinical samples. IA and MV analysed data. IA,  
347 MV and SSP wrote the manuscript with contributions from all authors.

348 **Conflict of interests:** The authors declare no competing financial interests.

349

350 **References**

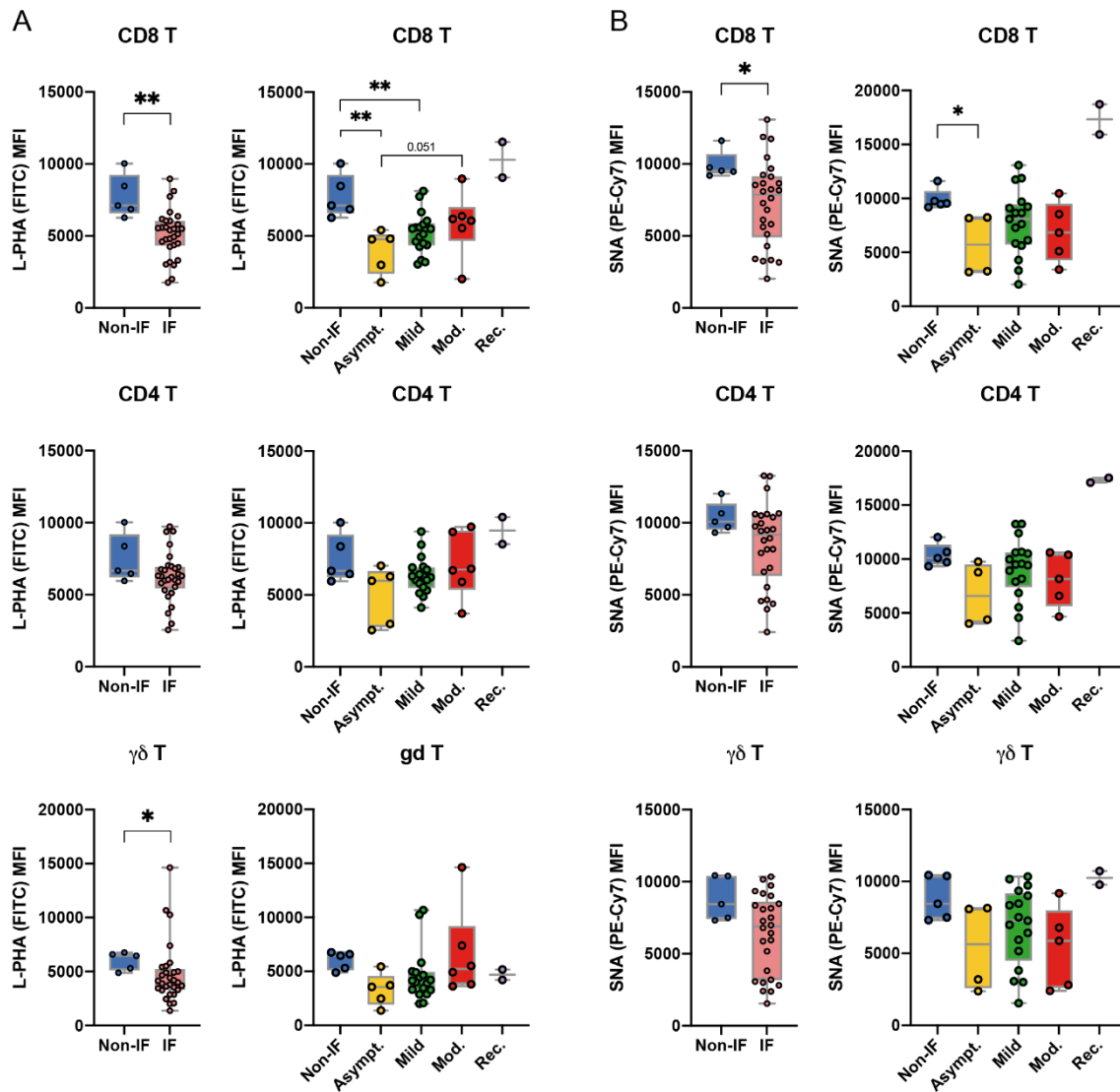
- 351 1. WHO. Dashboard | WHO Coronavirus Disease (COVID-19). .
- 352 2. Dong, E., H. Du, and L. Gardner. 2020. An interactive web-based dashboard to track  
353 COVID-19 in real time. *Lancet. Infect. Dis.* 20: 533–534.
- 354 3. Wu, Z., and J. M. McGoogan. 2020. Characteristics of and Important Lessons From  
355 the Coronavirus Disease 2019 (COVID-19) Outbreak in China: Summary of a Report of  
356 72 314 Cases From the Chinese Center for Disease Control and Prevention. *JAMA* 323:  
357 1239–1242.
- 358 4. Baden, L. R., H. M. El Sahly, B. Essink, K. Kotloff, S. Frey, R. Novak, D. Diemert,  
359 S. A. Spector, N. Rouphael, C. B. Creech, J. McGettigan, S. Kehtan, N. Segall, J. Solis,  
360 A. Brosz, C. Fierro, H. Schwartz, K. Neuzil, L. Corey, P. Gilbert, H. Janes, D.  
361 Follmann, M. Marovich, J. Mascola, L. Polakowski, J. Ledgerwood, B. S. Graham, H.  
362 Bennett, R. Pajon, C. Knightly, B. Leav, W. Deng, H. Zhou, S. Han, M. Ivarsson, J.  
363 Miller, T. Zaks, and COVE Study Group. 2020. Efficacy and Safety of the mRNA-1273  
364 SARS-CoV-2 Vaccine. *N. Engl. J. Med.*
- 365 5. Polack, F. P., S. J. Thomas, N. Kitchin, J. Absalon, A. Gurtman, S. Lockhart, J. L.  
366 Perez, G. Pérez Marc, E. D. Moreira, C. Zerbini, R. Bailey, K. A. Swanson, S.  
367 Roychoudhury, K. Koury, P. Li, W. V Kalina, D. Cooper, R. W. Frenck, L. L. Hammitt,  
368 Ö. Türeci, H. Nell, A. Schaefer, S. Ünal, D. B. Tresnan, S. Mather, P. R. Dormitzer, U.  
369 Şahin, K. U. Jansen, W. C. Gruber, and C4591001 Clinical Trial Group. 2020. Safety  
370 and Efficacy of the BNT162b2 mRNA Covid-19 Vaccine. *N. Engl. J. Med.* 383: 2603–  
371 2615.
- 372 6. Guan, W., Z. Ni, Y. Hu, W. Liang, C. Ou, J. He, L. Liu, H. Shan, C. Lei, D. S. C.  
373 Hui, B. Du, L. Li, G. Zeng, K.-Y. Yuen, R. Chen, C. Tang, T. Wang, P. Chen, J. Xiang,  
374 S. Li, J. Wang, Z. Liang, Y. Peng, L. Wei, Y. Liu, Y. Hu, P. Peng, J. Wang, J. Liu, Z.  
375 Chen, G. Li, Z. Zheng, S. Qiu, J. Luo, C. Ye, S. Zhu, and N. Zhong. 2020. Clinical  
376 Characteristics of Coronavirus Disease 2019 in China. *N. Engl. J. Med.* 382: 1708–  
377 1720.
- 378 7. Laing, A. G., A. Lorenc, I. del Molino del Barrio, A. Das, M. Fish, L. Monin, M.  
379 Muñoz-Ruiz, D. R. McKenzie, T. S. Hayday, I. Francos-Quijorna, S. Kamdar, M.  
380 Joseph, D. Davies, R. Davis, A. Jennings, I. Zlatareva, P. Vantourout, Y. Wu, V. Sofra,  
381 F. Cano, M. Greco, E. Theodoridis, J. Freedman, S. Gee, J. N. E. Chan, S. Ryan, E.

- 382 Bugallo-Blanco, P. Peterson, K. Kisand, L. Haljasmägi, L. Chadli, P. Moingeon, L.  
383 Martinez, B. Merrick, K. Bisnauthsing, K. Brooks, M. A. A. Ibrahim, J. Mason, F.  
384 Lopez Gomez, K. Babalola, S. Abdul-Jawad, J. Cason, C. Mant, J. Seow, C. Graham,  
385 K. J. Doores, F. Di Rosa, J. Edgeworth, M. Shankar-Hari, and A. C. Hayday. 2020. A  
386 dynamic COVID-19 immune signature includes associations with poor prognosis. *Nat.*  
387 *Med.* 1–13.
- 388 8. Zhou, R., K. K.-W. To, Y.-C. Wong, L. Liu, B. Zhou, X. Li, H. Huang, Y. Mo, T.-Y.  
389 Luk, T. T.-K. Lau, P. Yeung, W.-M. Chan, A. K.-L. Wu, K.-C. Lung, O. T.-Y. Tsang,  
390 W.-S. Leung, I. F.-N. Hung, K.-Y. Yuen, and Z. Chen. 2020. Acute SARS-CoV-2  
391 Infection Impairs Dendritic Cell and T Cell Responses. *Immunity* 53: 864–877.
- 392 9. Lucas, C., P. Wong, J. Klein, T. B. R. Castro, J. Silva, M. Sundaram, M. K.  
393 Ellingson, T. Mao, J. E. Oh, B. Israelow, T. Takahashi, M. Tokuyama, P. Lu, A.  
394 Venkataraman, A. Park, S. Mohanty, H. Wang, A. L. Wyllie, C. B. F. Vogels, R.  
395 Earnest, S. Lapidus, I. M. Ott, A. J. Moore, M. C. Muenker, J. B. Fournier, M.  
396 Campbell, C. D. Odio, A. Casanovas-Massana, R. Herbst, A. C. Shaw, R. Medzhitov,  
397 W. L. Schulz, N. D. Grubaugh, C. Dela Cruz, S. Farhadian, A. I. Ko, S. B. Omer, and  
398 A. Iwasaki. 2020. Longitudinal analyses reveal immunological misfiring in severe  
399 COVID-19. *Nature* 584: 463–469.
- 400 10. Mehta, P., D. F. McAuley, M. Brown, E. Sanchez, R. S. Tattersall, J. J. Manson, and  
401 U. HLH Across Speciality Collaboration. 2020. COVID-19: consider cytokine storm  
402 syndromes and immunosuppression. *Lancet (London, England)* 395: 1033–1034.
- 403 11. Pereira, M. S., I. Alves, M. Vicente, A. Campar, M. C. Silva, N. A. Padrão, V.  
404 Pinto, Â. Fernandes, A. M. Dias, and S. S. Pinho. 2018. Glycans as Key Checkpoints of  
405 T Cell Activity and Function. *Front. Immunol.* 9: 2754.
- 406 12. Varki, A., R. D. Cummings, J. D. Esko, P. Stanley, G. W. Hart, M. Aebi, A. G.  
407 Darvill, T. Kinoshita, N. H. Packer, J. H. Prestegard, R. L. Schnaar, and P. H.  
408 Seeberger. 2015. *Essentials of Glycobiology*. Cold Spring Harbor Laboratory Press.
- 409 13. Dias, A. M., A. Correia, M. S. Pereira, C. R. Almeida, I. Alves, V. Pinto, T. A.  
410 Catarino, N. Mendes, M. Leander, M. T. Oliva-Teles, L. Maia, C. Delerue-Matos, N.  
411 Taniguchi, M. Lima, I. Pedroto, R. Marcos-Pinto, P. Lago, C. A. Reis, M. Vilanova, and  
412 S. S. Pinho. 2018. Metabolic control of T cell immune response through glycans in

- 413 inflammatory bowel disease. *Proc. Natl. Acad. Sci. U. S. A.* 115: E4651–E4660.
- 414 14. Silva, M. C., Â. Fernandes, M. Oliveira, C. Resende, A. Correia, J. C. De-Freitas-  
415 Junior, A. Lavelle, J. Andrade-da-Costa, M. Leander, H. Xavier-Ferreira, J. Bessa, C.  
416 Pereira, R. M. Henrique, F. Carneiro, M. Dinis-Ribeiro, R. Marcos-Pinto, M. Lima, B.  
417 Lepenies, H. Sokol, J. C. Machado, M. Vilanova, and S. S. Pinho. 2020. Glycans as  
418 Immune Checkpoints: Removal of Branched N-glycans Enhances Immune Recognition  
419 Preventing Cancer Progression. *Cancer Immunol. Res.* 8: 1407–1425.
- 420 15. Ryan, S. O., and B. A. Cobb. 2012. Roles for major histocompatibility complex  
421 glycosylation in immune function. *Semin. Immunopathol.* 34: 425–41.
- 422 16. Demetriou, M., M. Granovsky, S. Quaggin, and J. W. Dennis. 2001. Negative  
423 regulation of T-cell activation and autoimmunity by Mgat5 N-glycosylation. *Nature*  
424 409: 733–9.
- 425 17. Mkhikian, H., A. Grigorian, C. F. Li, H.-L. Chen, B. Newton, R. W. Zhou, C.  
426 Beeton, S. Torossian, G. G. Tatarian, S.-U. Lee, K. Lau, E. Walker, K. A. Siminovitch,  
427 K. G. Chandy, Z. Yu, J. W. Dennis, and M. Demetriou. 2011. Genetics and the  
428 environment converge to dysregulate N-glycosylation in multiple sclerosis. *Nat.*  
429 *Commun.* 2: 1–13.
- 430 18. Grigorian, A., S. Torossian, and M. Demetriou. 2009. T-cell growth, cell surface  
431 organization, and the galectin-glycoprotein lattice. *Immunol. Rev.* 230: 232–46.
- 432 19. Pereira, M. S., C. Durães, T. A. Catarino, J. L. Costa, I. Cleynen, M. Novokmet, J.  
433 Krištić, J. Štambuk, N. Conceição-Neto, J. C. Machado, R. Marcos-Pinto, F. Magro, S.  
434 Vermeire, G. Lauc, P. Lago, and S. S. Pinho. 2020. Genetic Variants of the MGAT5  
435 Gene Are Functionally Implicated in the Modulation of T Cells Glycosylation and  
436 Plasma IgG Glycome Composition in Ulcerative Colitis. *Clin. Transl. Gastroenterol.*  
437 11: e00166.
- 438 20. Van Breedam, W., S. Pöhlmann, H. W. Favoreel, R. J. de Groot, and H. J.  
439 Nauwynck. 2014. Bitter-sweet symphony: glycan–lectin interactions in virus biology.  
440 *FEMS Microbiol. Rev.* 38: 598–632.
- 441 21. Watanabe, Y., Z. T. Berndsen, J. Raghwani, G. E. Seabright, J. D. Allen, O. G.  
442 Pybus, J. S. McLellan, I. A. Wilson, T. A. Bowden, A. B. Ward, and M. Crispin. 2020.

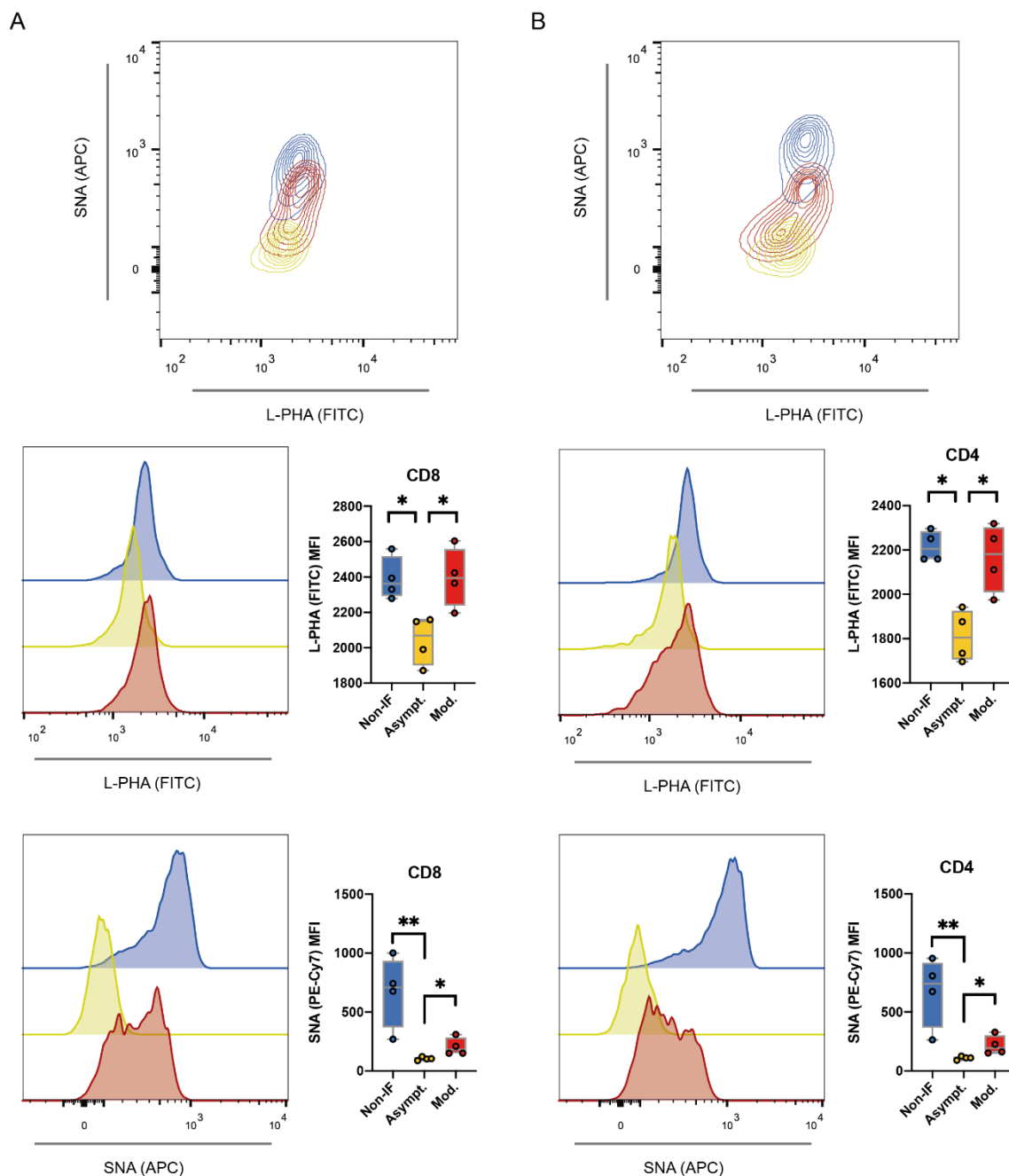
- 443 Vulnerabilities in coronavirus glycan shields despite extensive glycosylation. *Nat.*  
444 *Commun.* 11: 1–10.
- 445 22. Watanabe, Y., J. D. Allen, D. Wrapp, J. S. McLellan, and M. Crispin. 2020. Site-  
446 specific glycan analysis of the SARS-CoV-2 spike. *Science* 369: 330–333.
- 447 23. Marzi, A., T. Gramberg, G. Simmons, P. Möller, A. J. Rennekamp, M. Krumbiegel,  
448 M. Geier, J. Eisemann, N. Turza, B. Saunier, A. Steinkasserer, S. Becker, P. Bates, H.  
449 Hofmann, and S. Pöhlmann. 2004. DC-SIGN and DC-SIGNR interact with the  
450 glycoprotein of Marburg virus and the S protein of severe acute respiratory syndrome  
451 coronavirus. *J. Virol.* 78: 12090–5.
- 452 24. Amraie, R., M. A. Napoleon, W. Yin, J. Berrigan, E. Suder, G. Zhao, J. Olejnik, S.  
453 Gummuluru, E. Muhlberger, V. Chitalia, and N. Rahimi. 2020. CD209L/L-SIGN and  
454 CD209/DC-SIGN act as receptors for SARS-CoV-2 and are differentially expressed in  
455 lung and kidney epithelial and endothelial cells. *bioRxiv* 2020.06.22.165803.
- 456 25. Grigorian, A., H. Mkhikian, and M. Demetriou. 2012. Interleukin-2, Interleukin-7, T  
457 cell-mediated autoimmunity, and N-glycosylation. *Ann. N. Y. Acad. Sci.* 1253: 49–57.
- 458 26. Dias, A. M., J. Dourado, P. Lago, J. Cabral, R. Marcos-Pinto, P. Salgueiro, C. R.  
459 Almeida, S. Carvalho, S. Fonseca, M. Lima, M. Vilanova, M. Dinis-Ribeiro, C. A. Reis,  
460 and S. S. Pinho. 2014. Dysregulation of T cell receptor N-glycosylation: a molecular  
461 mechanism involved in ulcerative colitis. *Hum. Mol. Genet.* 23: 2416–27.
- 462 27. Bagriaciik, E. U., and K. S. Miller. 1999. Cell surface sialic acid and the regulation  
463 of immune cell interactions: the neuraminidase effect reconsidered. *Glycobiology* 9:  
464 267–75.
- 465 28. Demetriou, M., M. Granovsky, S. Quaggin, and J. W. Dennis. 2001. Negative  
466 regulation of T-cell activation and autoimmunity by Mgat5 N-glycosylation. *Nature*  
467 409: 733–739.
- 468 29. Pappu, B. P., and P. A. Shrikant. 2004. Alteration of cell surface sialylation  
469 regulates antigen-induced naive CD8+ T cell responses. *J. Immunol.* 173: 275–84.
- 470 30. Thevarajan, I., T. H. O. Nguyen, M. Koutsakos, J. Druce, L. Caly, C. E. van de  
471 Sandt, X. Jia, S. Nicholson, M. Catton, B. Cowie, S. Y. C. Tong, S. R. Lewin, and K.

- 472 Kedzierska. 2020. Breadth of concomitant immune responses prior to patient recovery:  
473 a case report of non-severe COVID-19. *Nat. Med.* 26: 453–455.
- 474 31. Matzinger, P. 2002. The danger model: a renewed sense of self. *Science* 296: 301–5.
- 475 32. Long, Q.-X., X.-J. Tang, Q.-L. Shi, Q. Li, H.-J. Deng, J. Yuan, J.-L. Hu, W. Xu, Y.  
476 Zhang, F.-J. Lv, K. Su, F. Zhang, J. Gong, B. Wu, X.-M. Liu, J.-J. Li, J.-F. Qiu, J. Chen,  
477 and A.-L. Huang. 2020. Clinical and immunological assessment of asymptomatic  
478 SARS-CoV-2 infections. *Nat. Med.* 26: 1200–1204.
- 479 33. Pérez-Cabezas, B., R. Ribeiro, I. Costa, S. Esteves, A. R. Teixeira, T. Reis, R.  
480 Monteiro, A. Afonso, V. Pinheiro, M. I. Antunes, M. L. Araújo, J. N. Ribeiro, A.  
481 Cordeiro-da-Silva, N. Santarém, and J. Tavares. 2021. IL-2 and IFN- $\gamma$  are biomarkers of  
482 SARS-CoV-2 specific cellular response in whole blood stimulation assays. *medRxiv*  
483 2021.01.04.20248897.
- 484 34. van Kooyk, Y., and G. A. Rabinovich. 2008. Protein-glycan interactions in the  
485 control of innate and adaptive immune responses. *Nat. Immunol.* 9: 593–601.
- 486 35. Netea, M. G., E. J. Giamarellos-Bourboulis, J. Domínguez-Andrés, N. Curtis, R. van  
487 Crevel, F. L. van de Veerdonk, and M. Bonten. 2020. Trained Immunity: a Tool for  
488 Reducing Susceptibility to and the Severity of SARS-CoV-2 Infection. *Cell* 181: 969–  
489 977.
- 490 36. Luo, M., J. Liu, W. Jiang, S. Yue, H. Liu, and S. Wei. 2020. IL-6 and CD8+ T cell  
491 counts combined are an early predictor of in-hospital mortality of patients with COVID-  
492 19. *JCI Insight* 5.
- 493

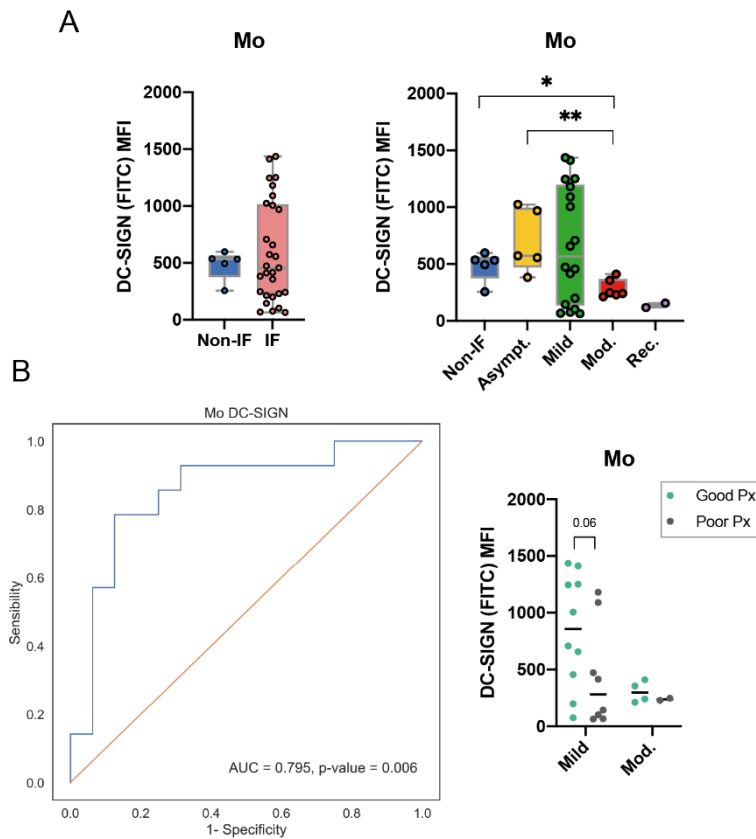


494

495 **Fig.1** – Peripheral T cell glycoprofile is altered upon SARS-CoV-2 infection at  
 496 diagnosis. Levels (Mean intensity fluorescence, MFI) of (A) L-PHA lectin binding,  
 497 detecting  $\beta$ 1,6-GlcNAc branched *N*-glycans and (B) SNA lectin binding, detecting  $\alpha$ -2,6  
 498 sialylation, in CD8<sup>+</sup>, CD4<sup>+</sup> and  $\gamma\delta$  T cell subsets of non-infected donors (Non-IF; n=5)  
 499 and infected (IF; n=30) patients. Levels of (A) L-PHA and (B) SNA lectin binding for  
 500 each disease severity group: asymptomatic (Asympt.;n=5), mild (n=18), moderate  
 501 (Mod.; n=6) and recovered (Rec; n=2) Each dot represents one patient. Mann-Whitney  
 502 t-test was performed to evaluate statistically significance differences between each  
 503 group-pair. \*  $p$ -value<0.05, \*\*<0.005.



504  
 505 Figure 2 – Patient-derived serum induces a differential T cell glycosylation comparing  
 506 asymptomatic and symptomatic patients (A) L-PHA lectin and (B) SNA lectin binding  
 507 (MFI) of CD8<sup>+</sup> and CD4<sup>+</sup> T cells from a healthy donor, independent of our cohort,  
 508 incubated for 24-hours with 10% plasma from 4 patients from each group (Non-IF,  
 509 asymptomatic or moderate). Each dot represents a subject. Gating strategies for each  
 510 population are included in **Supplemental Figure 1A**. Mann-Whitney t-test was  
 511 performed to evaluate statistically significance differences between each group-pair. \*  
 512 *p*-value<0.05, \*\*<0.005.



513

514 Fig.3 – DC-SIGN expression in peripheral monocytes as a predictor of good vs. poor  
515 prognosis in COVID-19 patients. **(A)** Levels of DC-SIGN surface expression (MFI) in  
516 monocytes (Mo). **(B)** Receiver operating characteristic (ROC) curve plotted for the DC-  
517 SIGN expression levels in monocytes from COVID-19 patients. The distribution of DC-  
518 SIGN levels are represented regarding the prognosis, Px, (day 14; good Px in green and  
519 poor Px in grey) as well as the severity at diagnosis. Each dot represents one patient  
520 N=24. Gating strategies for each population are included in **Supplemental Figure 1A**.  
521 Mann-Whitney t-test was performed to evaluate statistically significance differences. \*  
522  $p$ -value < 0.05, \*\* < 0.005, or represented.

523